DESIGN, ANALYSIS AND DEVELOPMENT OF BRACKETS EXHIBITING SNAP THROUGH BUCKLING BEHAVIOR

by

Surya Phani Krishna Nukala

A dissertation submitted to the faculty of
The University of North Carolina at Charlotte
in partial fulfillment of the requirements
for the degree of Masters of Science in
Mechanical Engineering

Charlotte

2017

Approved by:

Dr. Peter Tkacik

Dr. Jerry Hill

Dr. Russell Keanini

ABSTRACT

SURYA PHANI KRISHNA NUKALA. Design, Analysis and Development of Brackets Exhibiting Snap Through Buckling Behavior.
(Under the direction of DR. PETER TKACIK)

Support structures act as the back bone to the effective functionality of any system. Strength, stiffness and durability are the main contributing factors for a robust structure. But, sometimes it is important for a support structure to exhibit sufficient deflection under the application of load to avoid excessive load transmission towards the weak links of the structure.

With the fore mentioned requirement as the motivation, a load supporting bracket has been designed and developed for a special purpose application of allowing maximum deformation without failing beyond a threshold load criteria. Such a requirement can be achieved by designing a spring loaded mechanism which would collapse beyond certain load and retract as and when the load is released. Design of such mechanisms involves high number of parts and also demand frequent service of the parts to ensure fail proof functionality.

This thesis report describes the development of simple structure which capitalizes the snap-through buckling behavior of materials within their elastic limit. A comprehensive methodology of the design of structure and working is presented using the CAD.The design is tested using both computational method and on field testing. In conclusion, a collapsible structure for the special purpose industrial application is designed, developed and tested to meet the requirements laid down by Michelin Inc.

DEDICATION

To my parents, my advisor, Michelin Inc. and my friends for being a great source of support throughout this journey.

ACKNOWLEDGMENTS

First and foremost, I would like to thank my advisor and professor at UNC Charlotte Dr. Peter Tkacik and Calivin Bradley from Michilen Inc. for providing me with a wonderful opportunity of working on a real time project. Also, on a special note I would like to thank Stuart Gambill my fellow master's student at UNC Charlotte, for helping me through out the project both morally and technically. I would like to take this opportunity to thank Franklin Green from UNC Charlotte for teaching to operate the instron test machine and test few material samples. Also, I would like to thank Jerry Dahlberg for his extended support throughout the course of this project.

My sincere thanks also goes to my friends and room mates who have been a family away from family. They helped to keep a lively social atmosphere around me alongside my tight schedule. Last but not the least, I thank my family for supporting me both morally and financially to complete my Masters education.

TABLE OF CONTENTS

LIST OF TABLES

LIST OF FIGURES

CHAPTER 1: INTRODUCTION

1.1 Product development

Development of product is a broad engineering domain problem involving design, test, manufacture and deliver. A collective development of all the fore said stages of crucial for smooth development flow process.

Identification of the problem and choosing a right method and path to solve it is crucial for to provide a design solution. The design problem solved in this thesis addresses designing of product, testing its functionality, manufacturing procedure and assembly method. Hence the path followed must ensure parallel development of all the process closely matching concurrent engineering.

1.2 Organization of Thesis

Chapter 2 describes the Problem statement and basic buckling phenomenon

Chapter 3 presents the development of the conceptual design and dives further in to selecting a design from various concepts with the help of morphological charts.

Chapter 4 includes development of proof of concept for the developed concept design.

Chapter 5 deals with Preliminary Design, Manufacturing method and Testing of the selected conceptual design.

Chapter 6 deals with Detailed Design and Manufacturing procedure.

Chapter 7 give a brief introduction of mathematics behind the non linear finite element analysis employed to study buckling behavior.

Chapter 8 shows the Finite Element Analysis of the above design and depicts relation between the section modulus of the part.

Chapter 9 enlists the concluding arguments

CHAPTER 2: PROBLEM STATEMENT AND BASICS OF BUCKLING

2.1 Problem Statement

Support structures act as the back bone to the effective functionality of any system. Strength, stiffness and durability are the main contributing factors for a robust structure. But, sometimes it is important for a support structure to exhibit sufficient deflection under the application of load to avoid excessive load transmission towards the weak links of the structure and reduce the possibility of failure due to high stresses.

To fulfill the fore mentioned requirement, a load supporting bracket has been designed and developed for a special purpose application of allowing maximum deformation without failing beyond a threshold load criteria. Such a load which is to act beyond the threshold limit acts on the structure due sudden impact between two connecting parts.

The failure which in this context is cracking of structure during is regular operational cycles. Such a failure will result in parts coming of loose to damage the personal and property in its vicinity. The new bracket replaces already existing bracket (shown in Figure 2.1 1) to enhance the functionality of the system.

Considering the need to keep secrecy for the industry sponsoring for the project, the parts that are being supported by the designed brackets is not disclosed in the report. The part on which the support structure is rests and is fastened to is referred to as base labeled as 1a in Figure 2.1 and the parts which are supported by the bracket are referred to as load bearing component. These notations are followed for the entire report.

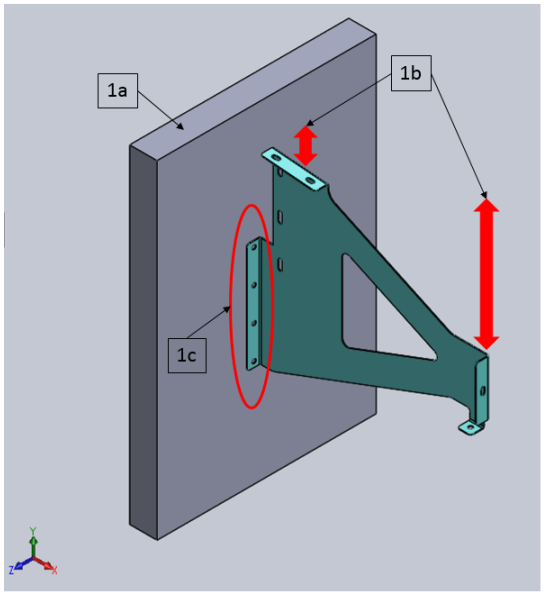

Figure 2.1: 1a.Base on which the bracket rests. 1b. Direction and location of the load being applied on the bracket. 1c. Location at which the bracket is attached to the base

Based on the nature of the attachment of the load bearing component whose parameters are fixed, it is observed that the load is applied in "Y-Direction" of the Cartesian coordinate system as shown as 1b in Figure 2.1.

2.2 Buckling and Snap through buckling

2.2.1 Buckling

When a structure is subjected to compressive stresses (considering axial direction alone), there can be a possibility of sudden sideways deflection of the structural member which is characterized as buckling. In theoretical science point of view, buckling is a mathematical instability that leads to a failure mode. This phenomenon can occur even when the stresses in the structure are way below yield criteria of the material [11].

Considering a long column subjected to compressive load as shown in the Figure

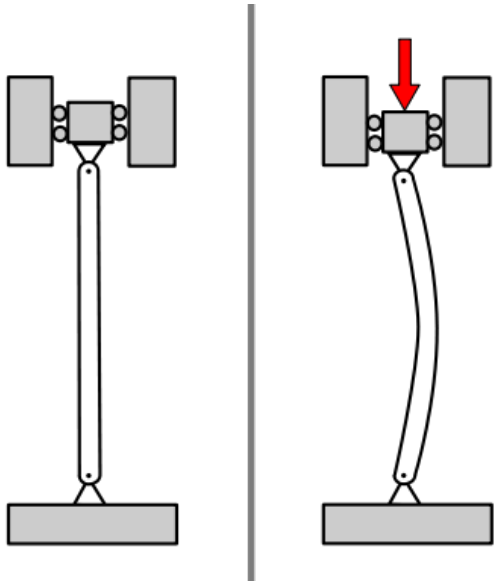

Figure 2.2: Column Buckling

2.2,[11] . For such a problem in ideal world, the material is assumed to be isotropic without any defects and the load is applied exactly at center of the part leading to just compressive stresses. But, in reality material and geometric imperfections exist which result in the load being applied at an offset to the longitudinal axis of the column. As the load applied is increased on such a member, it will become large enough to make column unstable. Further loading beyond this threshold load results in unpredictable deflections in the column. If column is to support the load even after it has buckled such a phenomenon is called stable buckling behavior, else it is characterized as an unstable buckling behavior.

2.2.2 Snap through buckling

Under large displacements of the structures under buckling significantly changes the geometry of structure. Several factors such as material, connection defects, geometric defects and in particular buckling phenomenon may cause substantial reduction in load carrying capacity. Failure of a compression chord member may result in a large redistribution of force within the structure, without any increase in external

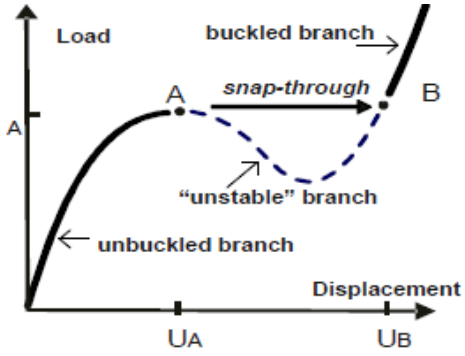

Figure 2.3: General load-displacement curve of a snap through buckling behavior.

load. If the structure were to remain stable the remaining members have to sustain loading borne by the structure. Such large displacements and redistribution of load to other members in the structure initially cause the collapse of the structure and head towards the next stable mode. Figure 2.3, [12] represents a general snap-through buckling behavior.

CHAPTER 3: CONCEPT GENERATION

3.1 Existing Design

Existing design for the system is shown in the Figure 2.1 and described in 2nd paragraph of Section 2.1.

3.1.1 Details of the existing design

As mentioned in section 2.1 and shown in the Figure 2.1 the load is applied in both positive and negative y direction of the axis system shown in the same figure. Considering the need to make the system stiff in the load application direction, area moment of inertia about x-axis (axis system refereed to in Figure 2.1) is designed to be maximum. The design was cut and fabricated out of aluminum sheet of thickness 2.3 mm (0.090 inches). Aluminum was chosen for the design to eliminate the possibility of galvanic corrosion of base material which is also made of aluminum.

3.1.2 Working under loading

Since the stiffness of the parts is very high in the y direction, the structure is reluctant to deform under loading. This results in high stress of the parts which are attached to the front end of bracket (i.e. locations 1b in Figure 2.1), resulting in failure of these attached parts. Also,buckling of the existing design about y-axis has 2 major issues

1. The angular direction of the buckling about y-axis cannot be controlled, i.e., the bracket can buckle either clockwise or anticlockwise about y axis.

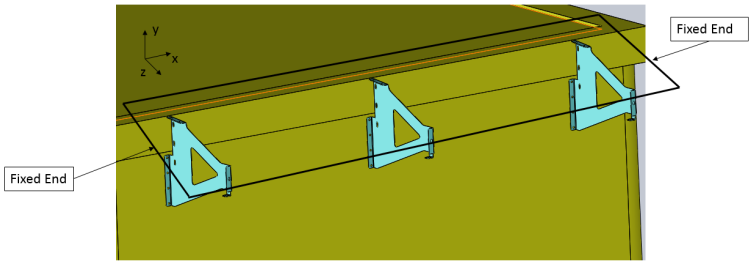

Figure 3.1: Schematic of Bracket and Load Attachment

2. The brackets do not operate independently. Three such brackets connect the load carrying component to the base as shown in Figure3.1.

   Figure 3.1 shows the schematic of how the load carrying component is attached to the brackets. The quadrilateral which encircles all the brackets is the load carrying component. The shorter ends of the component are attached to its adjacent structure to keep assembly intact. Such an assembly arises to two possible failure conditions:

   (a) If all the brackets buckle in the same direction, they tear the load applying structure the ends of the load applying structures causing an irreparable damage.

   (b) If the brackets buckle in different directions relative to each other, they tear the load applying structure in the middle of the cross section.

The above listed problems disqualify the minor modifications of the existing design to serve the purpose of high deflection under impact load.

3.2 Proposed Design

Proposed design uses 3 different brackets referred as "Rear Bracket", "Clicker Bracket" and "Front Bracket". These brackets are fastened together to complete the functionality of the supporting structure as shown in the figure 3.2.

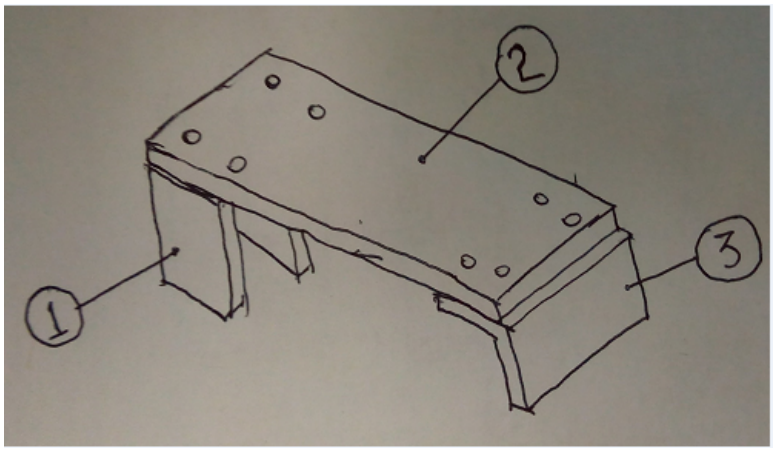

Figure 3.2: Assembly of the Concept. 1- Rear Bracket, 2-Clicker Bracket,3- Front Bracket

3.2.1 Working

The rear bracket and front bracket attach the clicker bracket to base and load respectively. Clicker bracket is the only component in the complete assembly which buckles under loading. When the system is loaded beyond a threshold limit, the clicker bracket buckles. The material with the clicker brackets are made, must have very high yield strength to avoid plastic deformation.

CHAPTER 4: MATERIAL SELECTION AND PROOF OF CONCEPT

4.1 Material Selection

The objective of the proposed design is to develop a part which can retract to its original shape when unloaded. Hence, a high strength material must be selected to suffice this requirement. Also, during the regular operations, the parts are exposed to sun light and other day to day weather conditions. Therefore, to effectively operate under these conditions, the material must show significant amount of resistance to corrosion. Additionally, as the parts have to be mass produced, ease of availability of material is also a driving factor.

Considering the fore mentioned requirements, the selection process narrowed down to aluminum and stainless steel. But, aluminum has very low yield strength and low fatigue life which makes it prone to plastic deformation and premature failure of components. Henceforth, the selection process moved forward with a wide research for various grades in stainless steel which posses high yield strength. Finally, Stainless Steel Grade 301 Full Hard material was chosen to design and develop clicker brackets. For front and rear brackets regular industrial grade aluminum of 2.3 mm (0.090 in.) sheet was chosen.

4.1.1 Properties of Stainless Steel 301 FH [1]

1. Equivalent grades

    - ASTM Designation - ASTM A666 Full Hard
    - UNS Designation - UNS 30100 Full Hard

2. Geometrical Properties

   - Type - Sheet
   - Thickness - 0.5 mm (0.020 in.)

3. Mechanical Properties

   - Density 7850 $\frac{kg}{m^3}$
   - Yield Strength - 965 MPa ($\frac{N}{mm^2}$)(140 KSI) [1]
   - Ultimate Tensile Strength - 1275 MPa ($\frac{N}{mm^2}$)(185 KSI) [1]
   - Percentage Elongation(in 50 mm or 2 in) - 9 %

4.2 Proof of Concept

The concept of the buckling behavior with in the elastic limit was tested to ensure the proof of concept for the proposed design. This proof was developed in multiple stages.

1. Retractable nature of the material
2. Controlling the location of buckling

1. Retractable nature of material when buckled was tested by bending long thin sheets of stainless steel and aluminum. The experimental test procedure is listed as follows

   - Aluminum
     (a) A flat sheet of 0.5 mm (0.02 inches) thick aluminum was cut to 300 mm (15 inches) in length and 50.8 mm (2 inches) wide.
     (b) The material was bent to collapse by fixing one end of the sheet to bench and other end pushed down manually.

(c) It was observed that the aluminum did not back to its original state.

(d) Another flat aluminum sheet with same dimensions mentioned in first point was cut and bent along its longitudinal axis into a 'V' shaped cross section with an included angle of 15 degrees.

(e) The specimen was bent and pushed down to buckle. The aluminum specimen did not revert back after releasing the load.

- Stainless Steel

  (a) A flat stainless steel sheet of 0.508 mm (0.02 inches) thick was cut to 300 mm (15 inches) in length and 50.8 mm (2 inches) wide.

  (b) The material was bent to collapse by fixing one end of the sheet to bench and other end pushed down manually.

  (c) It was observed that the steel sheet had returned back to its original state.

  (d) Another flat stainless sheet with same dimensions mentioned in first point was cut and bent along its longitudinal axis into a 'V' shaped cross section with an included angle of 15 degrees.

  (e) The specimen was bent and pushed down to buckle. The steel specimen reverted back after to its original shape when a small amount of load was applied in the opposite direction.

- Conclusion : It can be understood that due to higher yield stress of the stainless steel, the buckling phenomenon occurs way before the yield stress. Henceforth, the specimen reverts back to its original state upon smallest application of load in the opposite direction of buckling load.

2. Controlling buckling location:

- A flat stainless steel sheet of 2 inches wide and 15 inches long was cut and bent into a 'V' shape with included angle from 30 degrees.

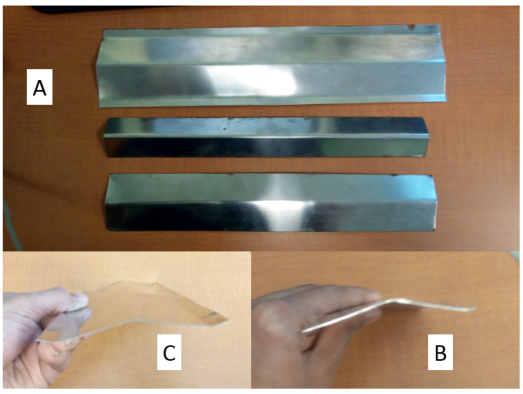

Figure 4.1: Specimen made to test buckling A.3 different cross section used for test. B. V type section. C. New section type

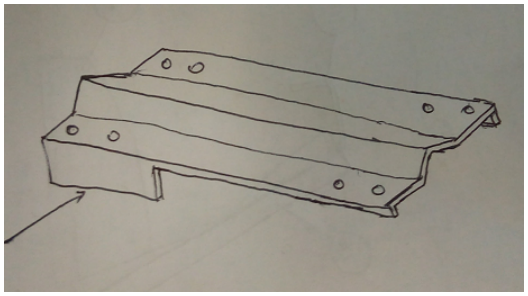

Figure 4.2: Base design for clicker bracket

- One end of the sheet was clamped and the load is applied at the other end. It was observed that the specimen buckles close to the support.
- Based on the above observation, the section modulus of the specimen was increased by changing the cross section at the support. This cross section is maintained from the end of the support to the 100 mm forward of the suppport. This design is tested and it was observed that the buckling was pushed forward by the same amount.

Conclusion :The from the results obtained from the basic experiments performed following choices have been made

1. Material for clicker bracket is Stainless Steel.
2. Figure 4.2 shows the shape of the concept on which further design will be based on.

CHAPTER 5: PRELIMINARY DESIGN, MANUFACTURING AND TESTING

Design concept of the clicker bracket obtained after the testing the proof of concept as shown in Figure 4.2 is used as the base for further design development. Also, sheet metal bending process with the press brake machine and cutting process with TorchMate plasma cutter act as the hard points for further design development.

5.1 Design

5.1.1 Clicker Bracket

Based on the results from the earlier experiments the section modulus of the clicker brackets is varied through out the length. Such a variation is achieved by changing the height of the flange along the length. The width of the clicker bracket is maintained to be 5 inches and length to be 16 inches. The 'V shaped 'central section is maintained constant through the length of the clicker bracket. Height of this central section is chosen as the design variable to vary the overall baseline stiffness of the component. The flanges drop down to the sides from both ends of the bracket and height of the flange drops down as the flange runs to the center. Central section for a length of 5 inches is the zone without any flanges which is potential zone for the part to undergo buckling. The clicker bracket has 4 holes at each end to fasten the part to front and rear stay. Figure 5.1 shows the preliminary design model of the bracket.

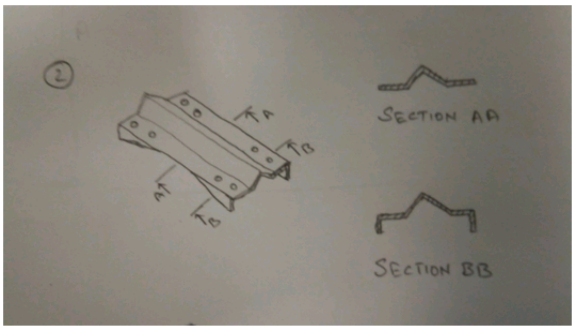

Figure 5.1: Preliminary Design of Clicker Bracket

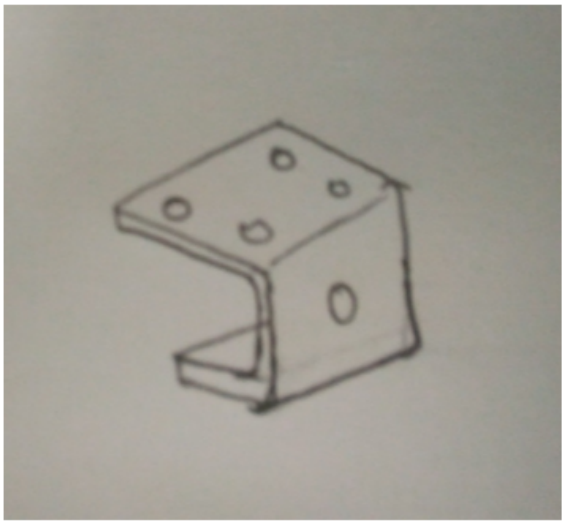

Figure 5.2: Preliminary Design of Front Bracket

5.1.2 Front Bracket

Front Bracket, is designed to be a C section when cut with XY plane. Vertical and the horizontal faces of the bracket are fastened to the load bearing structure and the angled face is attached to the clicker bracket. Clicker bracket is held from its lower side, thus limiting the width of the front bracket to 4.96. Front bracket is designed to limits in terms of width to provide maximum stiffness to the aluminum part. Figure 5.2 shows the preliminary design of the front bracket.

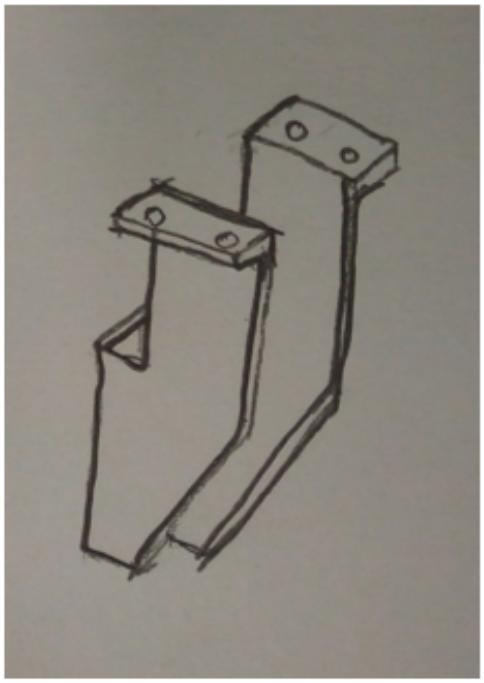

Figure 5.3: Preliminary Design of Rear Bracket

5.1.3 Rear Bracket

Rear bracket is mated with clicker bracket from its underside. Former part is riveted to the base on the middle face. Figure 5.3 shows the preliminary design of the rear bracket.

5.2 Manufacturing [2]

Manual shearing cutting method is not productive to cut 70 such parts (which is a requirement for Michelin). CNC plasma cutting method was chosen to cut raw material into unfolded work piece shape. Plasma cutter cuts through any conductive metal by accelerating hot plasma jet into the work piece. The head of the plasma cutter is moved with the help of the stepper motors along X Y and Z directions. These steppers motors are controlled by Accumove controller which takes CNC G-codes as the input to command stepper motors.

Table 5.1: Cutting parameters for Clicker brackets, Stay front and Stay rear

Parameter	Clicker Bracket	Stay Front & Stay Rear
Material	Stainless Steel 301 FH	Aluminum
Type	Sheet	Sheet
Thickness	0.508 mm	2.3 mm
Voltage	130 V	121 V
Current	45 A	45 A
Speed	9000 mm/min	8800 mm/min
Cut Height	1.5 mm	1.5 mm
Pierce Height	3.8 mm	3.8 mm

The CAD models for clicker, front and rear brackets are modeled and unfolded drawings for all the models were generated in DXF format using SolidWorks tool. These drawings were fed as in input to TorchMate VDM software to process the drawings and obtain G code. The G-code is fed into TorchMate Controller module to command stepper motors and cut the parts

Machine settings Since aluminum and stainless steel of different thickness are used, the machine settings have to be changed for each of them. The setting for each part are tabulated in table 5.1.

5.3 Testing

A simple test method to quickly test the parts and understand how the parts behave under buckling was designed

- Front bracket, clicker bracket and rear bracket were assembled together.
- Rear bracket was clamped to the bench using C-clamps to simulate a cantilever bending model.
- A push-pull gauge is hooked to the front bracket, and the assembly was pulled to bend the clicker bracket as shown in the Figure 5.4
- The load at which the parts buckle is tabulated and presented in Table 5.2

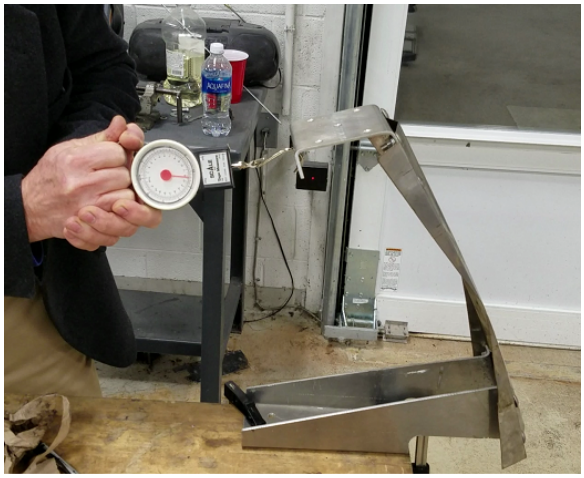

Figure 5.4: Preliminary Test Setup

Table 5.2: Preliminary Test Data

Test Number	Hill Height -mm(inch)	Upward Buckle -N(lbs)	Downward Buckle -N(lbs)
1	5.08(0.2)	88.9(20)	31.14(7)
2	5.08(0.2)	48.9(11)	31.14(7)
3	5.08(0.2)	48.9(11)	35.58(8)
4	5.08(0.2)	48.9(11)	35.58(8)
5	10.16(0.4)	111(25)	35.58(8)
6	25.4(1)	222+(50+)	222+(50+)

CHAPTER 6: DETAILED DESIGN AND MANUFACTURING

Proof of concept and preliminary design have laid a strong foundation for the development multiple domains of product development which include manufacturing and testing for this project. Experience and results from preliminary design, manufacturing and testing have shown potential problems which include

- Consistency in fabrication of clicker brackets. The bending angle of the hill section and symmetry about the longitudinal axis is key to ensure a consistent buckling load among all the brackets.
- Rear bracket designed for preliminary design prevents the clicker bracket from deflecting. Henceforth the rear bracket design had to be changed to increase local stiffness and make clicker bracket the weakest link.
- Designed parts must fit under the envelope of the system.
- Minimum load carrying requirements listed in the Table 6.1.
- A robust test method had to be developed to ensure consistent test results.

Table 6.1: My caption

Force Direction	Top Panel
Avg. X Force(N)	-252.2
Avg. Y Force(N)	0.9
Avg. Z Force(N)	859.3

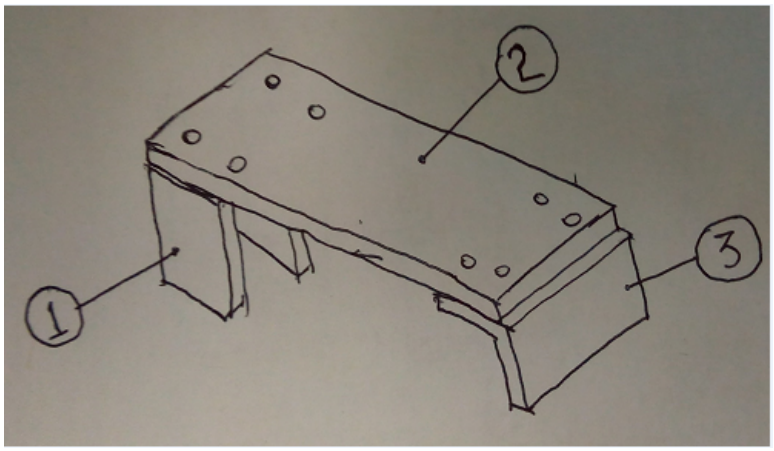

Figure 6.1: Assembly of the Concept. 1- Base Stay, 2-Clicker Bracket,3- Load Stay

6.1 Detailed Design

6.1.1 Front Bracket

Front Bracket Design

Brackets front had minimal number of problems through out the design process. The part had been optimized to have reduce the mass. A sequence of bending steps had been determined to ensure hassle free fabrication. The image of the front stay has been shown in the figure 6.2

The Figure 6.3 showing front view of the bracket front, highlights three major locations where material has been removed to reduce the mass of the bracket. Also, Figure 6.4 and Figure 6.5 highlight the assembly allowance of 6.35 mm (0.25 inches)to the load bearing component and clicker bracket respectively.

Front Bracket Fabrication

Front bracket was cut using the TorchMate plasma cutter available in UNCC Motor-sports Research Laboratory. Optimal machine parameters were determined during the preliminary design stage as show in Table 5.1. Sequence of fabricating

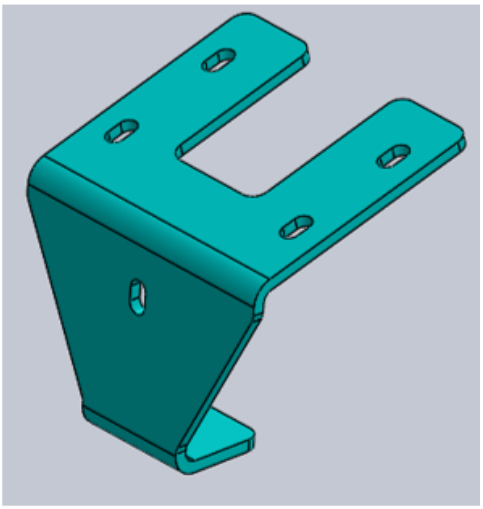

Figure 6.2: Bracket Front detailed design

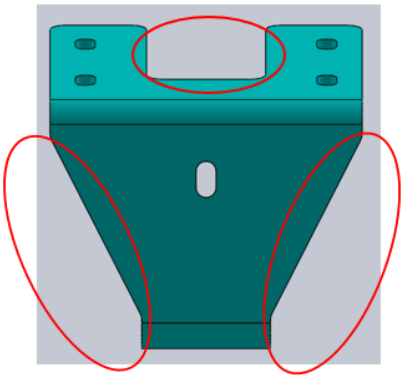

Figure 6.3: Front view of Front Bracket highlighting material removal.

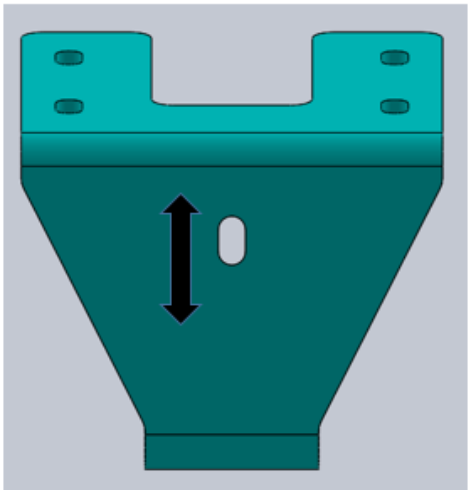

Figure 6.4: Front view of Front Bracket highlighting assembly allowance.

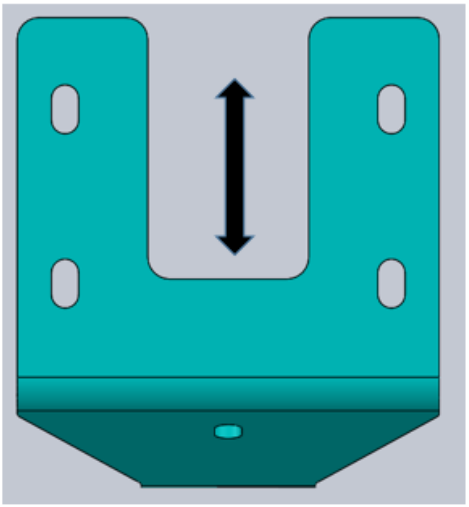

Figure 6.5: Top view of Front Bracket highlighting assembly allowance.

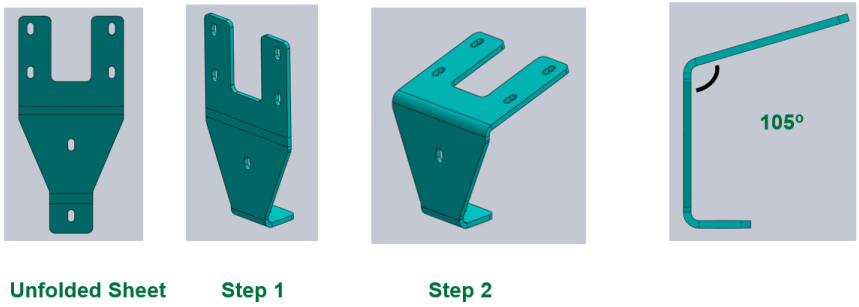

Figure 6.6: Sequence of operations to bend Bracket Front

operations include

- The parts are cut with the help of the plasma cutter.
- Edges of the cut part are smoothened using a pneumatic belt sander.
- With CAD drawings as reference, bend location markings were made on work piece.
- Portable hand bending machine shown in Figure 6.7 which was developed by John Martin an UNC Charlotte student was used to bend the parts. To bend parts in the hand bending machine, firstly the parts had to be clamped down on the bending machine while aligning the bend location marks to bend line.

Figure 6.7: Hand Bending Machine.

Then,the hand lever is pulled down to bend the part to its required bend angle. To ensure a hassle free bending operation, sequence of operations shown in Figure 6.6 are followed.

6.1.2 Rear Bracket

Rear Bracket Design

Bracket rear is the resting base for clicker bracket under loading. This is analogous to the fixed end of a cantilever beam. During the preliminary design test phases it was observed that bracket rear deflects under loading, thus reducing the clicker bracket from buckling. Figure 6.8 shows the bracket design in preliminary design phases highlighting the deflection of the bracket. To counter the problem the bracket design has been modified to increase the local stiffness of the part where the clicker bracket rests. Also, slots are made on the top instead of holes to allow for 6.35 mm(0.25 in.) of assembly allowance. The modified design of the bracket is as shown in the Figure 6.9.

Figure 6.8: Bracket Rear for preliminary design, highlighting deflection.

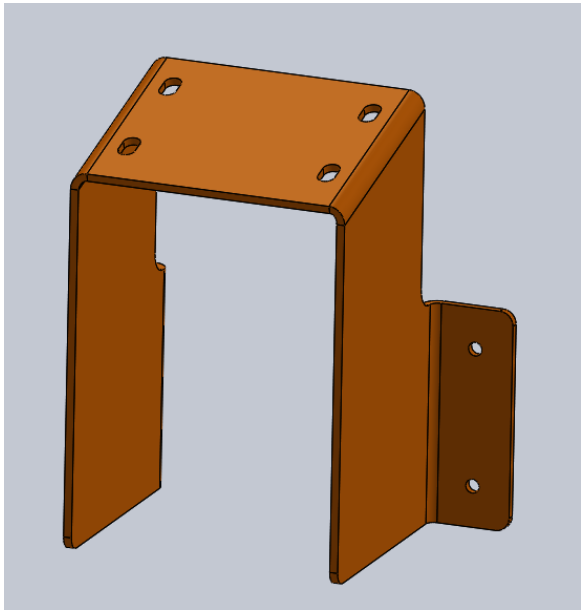

Figure 6.9: Bracket Rear for preliminary design, highlighting deflection.

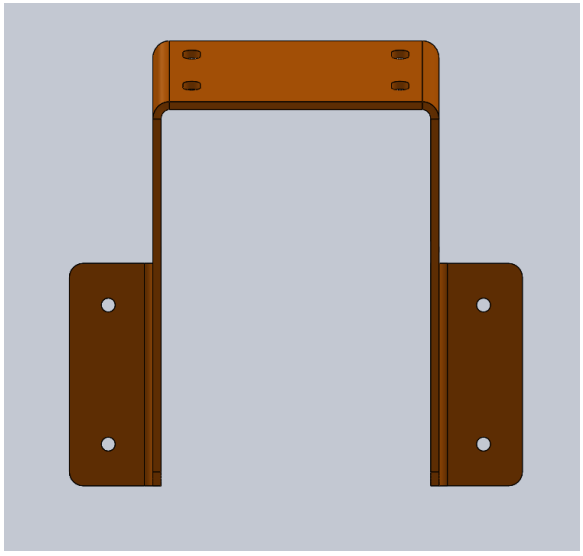

Figure 6.10: Front view of the rear bracket.

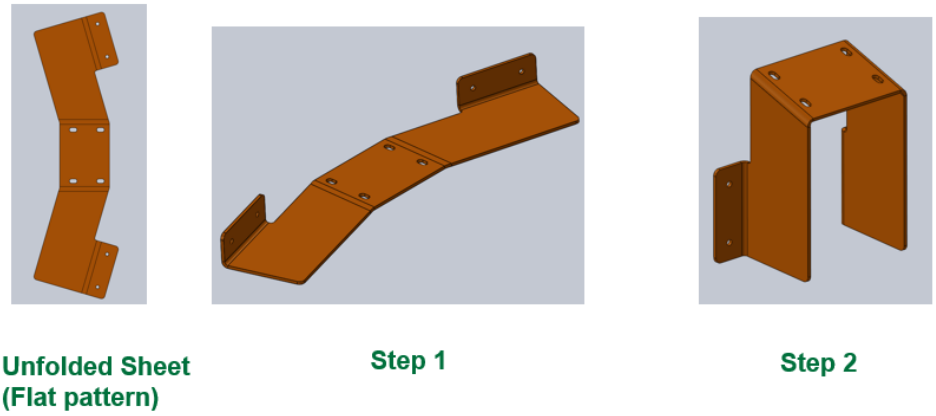

Figure 6.11: Sequence of bending operations of the rear bracket. Step 1: Bending done on 10 foot sheet-metal break. Step 2: Bending is done on custom made hand bending machine.

Rear Bracket Fabrication

Rear bracket was cut using the TorchMate plasma cutter. Optimal machine parameter which were determined during the preliminary design phase are show in Table 5.1. Sequence of operations include

- The parts are cut with the help of plasma cutter.
- Edges of the cut part are smoothened using a pneumatic belt sander.
- With CAD drawings as reference, bending location markings were made on work piece.
- Bending of rear bracket is done on two different machine to avoid self intersection of parts.
- Firstly, the left and right flanges of the bracket shown in Figure 6.10 are bent on the 10 foot braking machine.
- Then the part is shifted from the 10 foot brake machine to the custom made hand break machine. Part is clamped on to hand break machine and remaining two bends are completed. The sequence of bending operations is shown in the Figure 6.11

6.1.3 Clicker Bracket

Clicker Bracket Design

Clicker bracket has been developed to its fullest in the preliminary design stages. Final changes that were done to the design were to reduce the over all length of part to 392.4 mm (15.5 in.) to ensure that parts fit in the envelope. Also, the width of the part is maintained to be 132 mm (5.2 in).

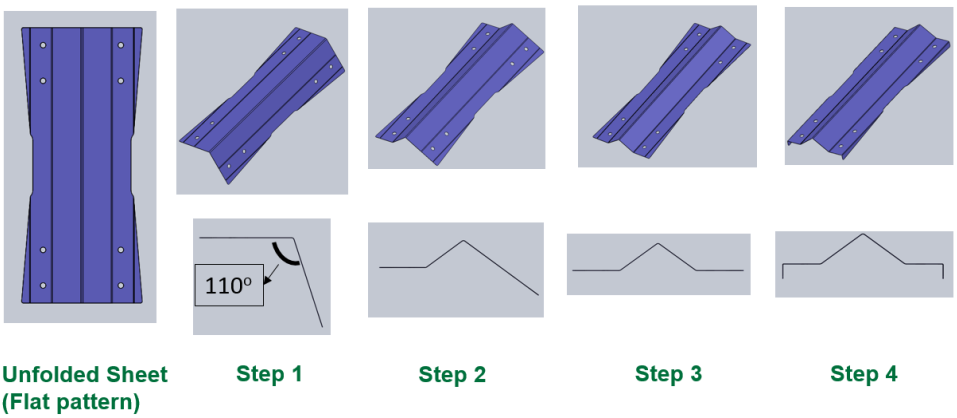

Figure 6.12: Sequence of bending operations of Clicker Bracket.

Clicker Bracket Fabrication

Sequence of operations for fabrication of clicker bracket include:

- The unfolded sheet or flat pattern is cut using plasma cutter.
- Edges of the cut part are de-burred using hand pneumatic sander.
- With CAD drawings as reference, bend locations were marked on work piece.
- Clicker brackets are bent with the help of the 10 foot sheet metal break machine.
- Sequence of bending operations are shown in the Figure 6.12.
- Flat pattern is aligned to the central marks and clamped in the sheet metal break machine. The lever is pulled to bend the part to 110°.
- In the Step 2 and Step 3, resting face bends are done.
- In the final step, bends are performed to make the flanges.

CHAPTER 7: INTRODUCTION TO COMPUTATIONAL METHOD

Buckling problem is a mathematical bifurcation problem which has to be solved using non linear solving techniques. Bifurcation theory is a mathematical study of a system whose output changes abruptly for small change in an input parameter of the system. Phenomenon of buckling under compressive axial loads observed in various civil structures, boilers, pistons of viscous dampers and hydraulic cylinders , and many more full under the category of bifurcation theory. For all the above listed problems beyond a threshold limit a small change in input load causes large deflections leading to loss of structure's load retaining capabilities. Solving such problems manually are cumbersome tasks. Henceforth, computational methods using finite element techniques are employed to estimate the critical buckling load of a system.

7.1 Finite Element Analysis Algorithm Followed

Finite element analysis is one of the many numerical methods which can solve a complex problem. Every finite element model follows three critical steps :

- Pre-processing: In this stage, the model is generated and all the properties which include material properties, geometrical properties and contact constraints. In a finite element method, the model is discretized into small elements connected at nodes. Finally a stiffness matrix is generated based on the above selections made.

- Analysis: The model prepared and meshed into fine elements is translated in a set of linear or non linear equations, to obtain displacement, temperature,

stress, strain, heat flux etc.

- Post-processing: The calculated output variables are correlated and plotted as a contours representing distribution of various parameters on the model.

  Abaqus 6.11 was used as one of the many available tools to solve the non-linear buckling problem.

7.2 Linear Eigenvalue Method [3],[4]

In a buckling problem, stability of a structure is analyzed by estimating the critical load. Critical load is usually calculated using linear eigenvalue analysis and is generally used for perfect structure.

$$F_{int} - \lambda F_{ext} = R(u) \tag{7.1}$$

F_{int} = Internal Forces

λ = Load Proportionality Factor

F_{ext} = External Forces

R(u) = Residual Stresses

Equation 7.1 is the general form for various mechanics problems which states that sum of internal forces developed due to stresses in an element and external forces must be equal to zero, i.e. R(u) = 0. This equation can be solved in multiple methods. Most well known method to solve the fore mentioned equation is linear eigenvalue method.

$$(K - \lambda K_t) * x = 0 \tag{7.2}$$

K = Stiffness matrix of the structure

K_t = Tangential stiffness of the structure

Equation 7.1 can be rewritten as equation 7.2 where K is the initial stiffness matrix of the structure and K_t is the tangential stiffness of the structure. Initial stiffness of the structure multiplied with displacement vector 'x' give rise to the internal forces in the structure. Tangential stiffness is the stiffness of the deformed structure when multiplied with displacement vector 'x' gives rise to external forces. For an eigenvalue problem, the mode λ and vector x for which K_t is zero is determined. All such modes and vectors which depict approximate load factor at which structure buckles and the mode shape respectively are listed. The lowest mode of above solution gives the lowest critical buckling load of the structure.

Limitations of Linear Eigenvalue analysis [4]

Linear eigenvalue problem works best for symmetrically loaded perfect structures which is mostly conservative in nature. But, no structure is perfect and posses imperfection either in material properties, geometrical properties or loading method. Due to such imperfections most of the structures buckle at a load, which is less than the load obtained from eigenvalue analysis.

Some structures which show a substantial stress distribution of stresses to change geometry collapse at a a load which is generally higher than the load estimated in an eigenvalue analysis. Such an uncertainty in this procedure makes it an secondary reference to draw a relative correlation between design parameters and critical buckling load.

Also, the eigenvector obtain from the solution is a relative displacement term with respect to a reference node. They do not depict the actual displacements and just provide the ratios of the displacement. Also, the stresses obtained are based on the scales of displacement. Henceforth, eigenvalue method is not suitable to predict critical buckling load for complex problems.

7.3 Newton-Raphson Method [5]

This method is mostly popularly used for many non linear finite element analysis problem. In Newton's method, the external load applied on the structure is gradually increased from a near zero value (0.001 time the actual load in Abaqus) to the desired external force. For ease of calculation the desired load remains constant and the load proportionality factor λ increase from near zero value to unity, thus controlling the load incrementation. At every increment the value of λ is slightly changed and determine the 'u' displacement vector. From equation 7.1 we can build the mathematical procedure as follows:

$$\lambda_1 = \lambda_0 + \Delta\lambda \tag{7.3}$$

Equation (7.3) calculates the λ values for the new increment.

$$u = u_0 + \Delta u \tag{7.4}$$

Equation (7.4) calculates the displacement vector 'u' for the new increment.

Hence, the residual load for the new increment in the Newton method can be written as

$$R(u_1) = R(u_0 + \Delta u) = F_{int}(u_0 + \Delta u) - (\lambda_0 + \delta\lambda) = 0 \tag{7.5}$$

where, $F_{int}(u_0 + \Delta u)$ is expanded using Taylor's series to obtain,

$$F_{int}(u_0 + \Delta u) = F_{int}(u_0) + [\frac{\partial F(u)}{\partial u}].\Delta u \tag{7.6}$$

and, $[\frac{\partial F(u)}{\partial u}] = [K_t]_{u_0}$

, which is called the tangent stiffness or the updated stiffness matrix at the new load

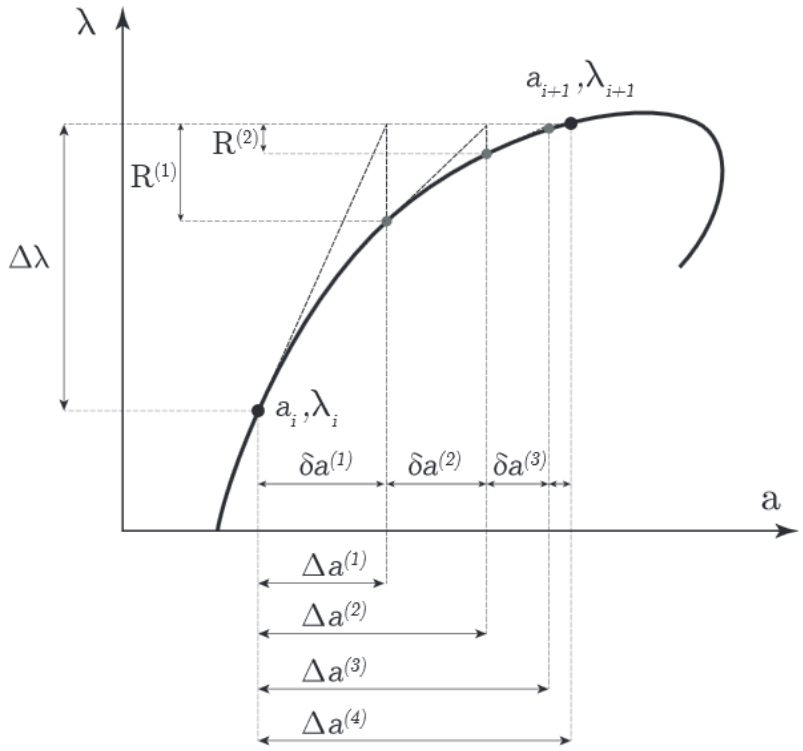

Figure 7.1: Graphical representation of Newton Raphson Method used to solve non linear Finite Element Problem.

increment.

$$\delta u = -[K_t]_{u_1}^{-1}.(\Delta\lambda F_{ext}) \tag{7.7}$$

$$\delta u = -[K_t]_{u_1}^{-1}.R(u_1) \tag{7.8}$$

Clubbing and mathematical manipulations of equations, the new displacement correction is obtained. This is added to the initial displacement to obtain new displacement. This iterative process is repeated over and again until the loop breaking criteria is met or the solver encounters an error. Graphical representation of the method is shown in the Figure 7.1

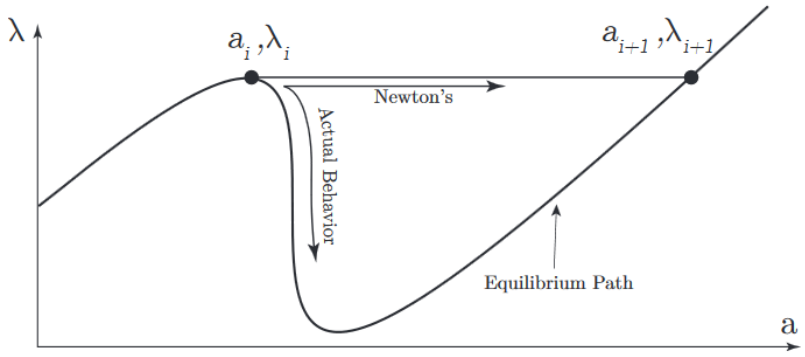

Figure 7.2: Graphical representation of limitations of Newton Raphson Method.

Limitations of Newton Raphson Method

This method estimates the critical buckling point but fails to predict the displacement behavior beyond the limit point a_i, λ_i, as shown in the Figure 7.2. This scenario occurs because $[K_t]$, tangent stiffness matrix becomes singular and is not positive definite after the collapse stage.

Hence, an even robust method call Arc length method is used to solve the buckling problems which can over come the problem of singularity and solving a non positive definite stiffness matrix.

7.4 Arc Length Method (Static Rik's Method) [5] [6]

The Arc-Length method is an efficient method in solving non-linear system of equations which exhibit one or more collapse points or critical points. In Newton-Raphson method, $\Delta\lambda$,smallest load increment, is known and Δu, smallest displacement increment was iteratively estimated. But, in Rik's method or arc length method both $\Delta\lambda$ and Δu are unknowns. To brief about this method,

$$R(u) = F_{int} - \lambda F_{ext} = 0 \tag{7.9}$$

Equation (7.9) is our equation of interest which has to be solved to obtain the

displacement as the output. If the point u_0 and λ_0 satisfy the equation (7.9) and $\Delta\lambda$ and Δu are the new increments in load factor and displacement respectively, equation (7.9) can be re-written as

$$R(u_1, \lambda_1) = F_{int}(u_0 + \Delta u) - \lambda F_{ext}(\lambda_0 + \Delta\lambda) = 0 \tag{7.10}$$

In general, the new chosen increment $(u_0 + \Delta u)$ and $(\lambda_0 + \Delta\lambda)$ do not lie on the load displacement curve and a correction factor in both load factor and displacement have to be introduced. With this new correction a new iteration has to be solved. This process is repeated until convergence is reached.

$$R(u_{11}, \lambda_{11}) = F_{int}(u_0 + \Delta u + \delta u) - F_{ext}(\lambda_0 + \Delta\lambda + \delta\lambda) = 0 \tag{7.11}$$

where, $\delta\lambda$ is the corrected load increment and δu is the corrected displacement.

Equation (7.11) is expanded using Taylor's series expansion and retaining just the linear range.

$$F_{int}(u_0 + \Delta u) + [\frac{\partial F_{int}(u)}{\partial u}].\delta u - (\lambda_0 + \Delta\lambda + \delta\lambda).F_{ext} = 0 \tag{7.12}$$

Where the partial differential of $F_{int}(u)$ with respect to u is call the Jacobian matrix of the system or the tangential stiffness matrix of the system.

$$[K_t]_{u_0+\Delta u}.\delta u - \delta\lambda F_{ext} = -[F_{int}(u_0 + \Delta u) - F_{ext}(\lambda_0 + \Delta\lambda)] = -R(u_1, \lambda_1) \tag{7.13}$$

Equation (7.13) has N equations and N+1 unknowns to be solved. Hence a supplementary equation called arc length equation is used to solve the above system of equations.

$$(\Delta u + \delta u)^T.(\Delta u + \delta u) + \Psi^2(\Delta\lambda + \delta\lambda)^2(F_{ext}^T.F_{ext}) = \Delta l^2. \tag{7.14}$$

In the equations (7.13) and (7.14), Ψ and Δl are user defined parameters, δu and $\delta\lambda$ are unknowns that have to be solved. To solve, the above system of equations, K_t becomes a sub matrix of a whole matrix system and it's singularity does not lead to errors. Henceforth, this method can be employed to study the buckling behavior in quasi-static state.

CHAPTER 8: FEA AND EXPERIMENTAL VALIDATION

Manual testing of parts designed during the preliminary design stage proved that, an effective testing method is important to effectively estimate critical buckling load of clicker bracket. As we increase the base stiffness of the part, it becomes difficult to test manually. Hence a robust test rig development is necessary to actual critical buckling load of the parts and compare them with finite element results.

8.1 Machine Description [7]

Instron universal test machine available in UNCC Motor-sports Research Lab was used to test the parts. The machine is equipped with a load cell rated 89000 N (20000 lb). The overall stroke length of the machine is 1 meters. This machine is a displacement controlled and the test bed moves at a specified speed which is referred as strain rate by the machine software. This test machine is it has enough room to install custom design test fixtures to test the parts as per operator's requirement. The operating methods of the machine are as follows

- The machine is turned on and the gauge length on the control panel is reset.
- The IEEE 488 connectivity is turned on to engage communication of test machine with computer.
- Instron X11 software installed on the computer is run.
- The test procedure that has to be performed is programmed on in that software and the method is saved.
- Multiple test runs can be conducted with the test procedure created.

Figure 8.1: Instron Test Machine UNCC Motor-sports Research Lab.

8.2 Fixture Design

To hold the clicker bracket assembly a custom test rig was designed to hold the bracket as it was held in its real time application. To accomplish this task in a cost effective way,

- 4 angle iron of 558.8 mm (22 in.) long were cut.
- Basic fabrication work is done to set up an L shaped fixture.

Figure 8.2: Fixture and bracket mounted on Instron test machine.

- Also, a plate of 203.2 mm x 152.4 mm (8 in. x 6 in.) was cut and bolted on the vertical legs of the L fixture.
- Assembled clicker bracket components are clamped on to the base plate mounted on L fixture.
- Now the clicker bracket assembly moves along with L fixtures and moving head of the machine.
- A square tube of 10" long was cut and welded to 6" x 6" x 0.25" C channel.
- This strut like structure is attached to the fixed end of the machine which records the reaction loads with the help of the load cell.
- Figure 8.2 shows the assembled test rig.

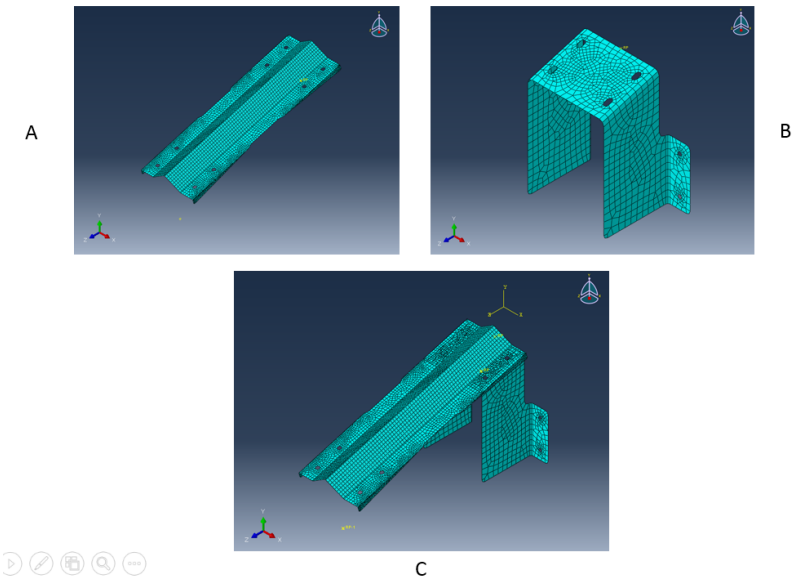

Figure 8.3: Meshed parts and assembly of the Finite Element Model. A - Clicker bracket meshed model, B - Rear bracket meshed model, C - Assembly of the meshed model.

8.3 Finite Element Analysis [8] [9] [10]

8.3.1 Model Preparation

Any Finite Element Analysis results must be validated with experimental results. Henceforth, a finite element model must be close to the experimental model to correlate data which help in predicting the results for a modified design. To approximately predict the critical buckling load of clicker bracket and estimate stress distribution on clicker bracket, rear bracket has been added to the model. Bracket front is eliminated to save computational space at time. Bracket rear has been added to the model as there is a significant contact interactions between bracket rear and clicker bracket which modify buckling load and stress distribution. To reduce computational time, rear bracket is modeled as a rigid part. Figure 8.3 shows the meshed geometry for analysis.

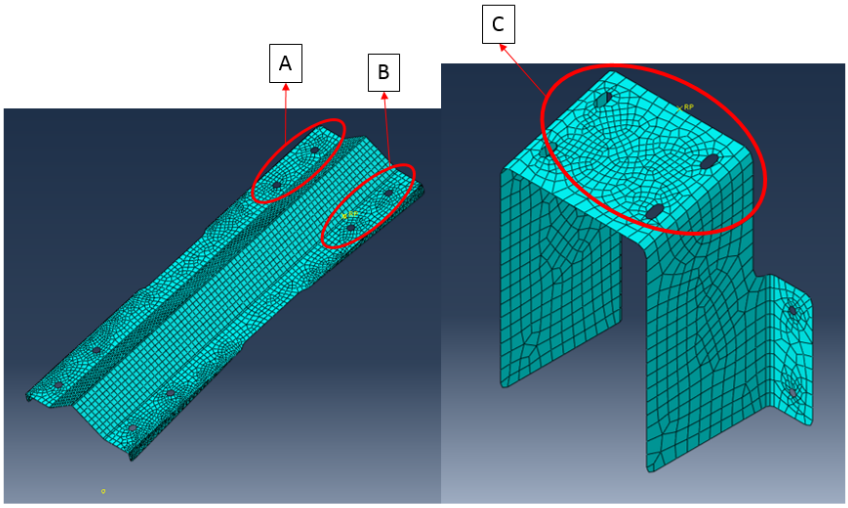

Figure 8.4: Meshed model of clicker bracket and rear bracket highlighting surface to surface contact. C and A and C and B are under surface to surface contact.

Contact Modeling Contact modeling plays a critical role in clearly understanding the buckling problem. Multiple iterations have been performed by to avoid contact problem and reduce the computational time. But, such a method has given rise to high stress singularities which disrupted complete stress distribution of model. Hence a contact interaction on surface of clicker bracket and rear bracket have been introduced as shown in the figure 8.4. Surface C of the rear bracket is chosen as the master surface and is independently in contact with the slave surfaces A and B of clicker bracket respectively.

Element Type Element type chosen is crucial for development of any finite element model. For this problem, a 4 Node Shell element with reduced integration S4R was chosen with an enhanced hourglass factor available on Abaqus is chosen. Shell element was chosen as the clicker bracket with very thin and the stresses in the thickness direction are assumed to be uniform. Advantage of shell element is that they provide best results for a small computational memory and time. Reduced integration element also serve the same purpose of saving memory and computational time as they calculate output quantities at fewer gauss points of an element. Since

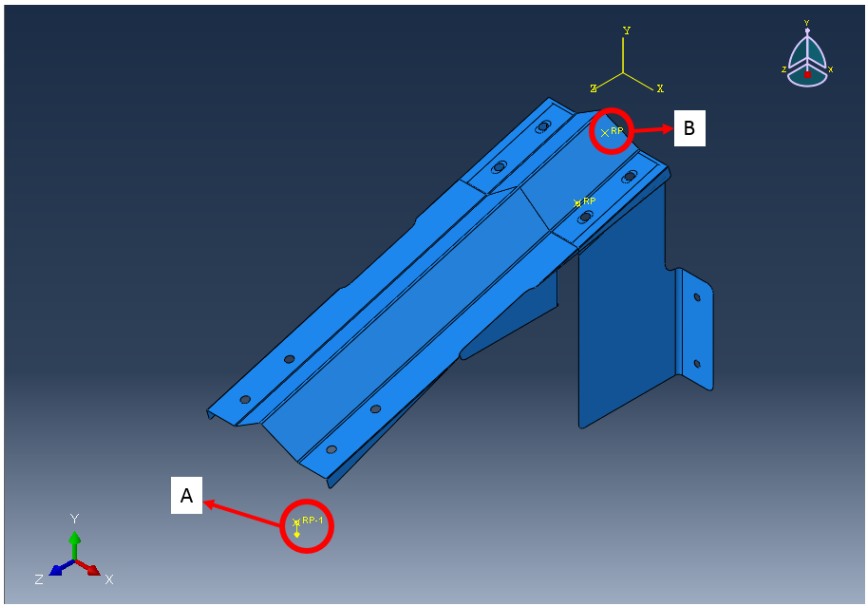

Figure 8.5: Assembly of finite element model highlighting load application point A and fixed point B

the problem deals with contact interaction, high elements might wrap or even get distorted. To prevent this problem enhance hourglass option was chosen based on various iterations performed.

Boundary Conditions Any second order partial differential equation must have at least two boundary conditions at two different time steps and locations to solve the problem. To simulate a real time application and match with experimental setup, a load of 1000 N is applied in negative y direction at reference point A as shown in the figure 8.5. Reference point B which represent rear bracket which is a rigid body has is all 6 DOF's constrained.

Results for Design 1 analysis [13] Figure 8.7 shows the load displacement curve obtained from finite element analysis of design iteration 1. From the graph it can be see that the clicker bracket gradually loses its ability to retain load beyond 928.2 Newtons. As the analysis is quasi-static in nature, the structure gradually loses it ability to retain load, rather than a sudden change. The limit point is achieved at 52^{nd} iteration of 250 iterations. The stress plot at 52^{nd} iteration is shown in the

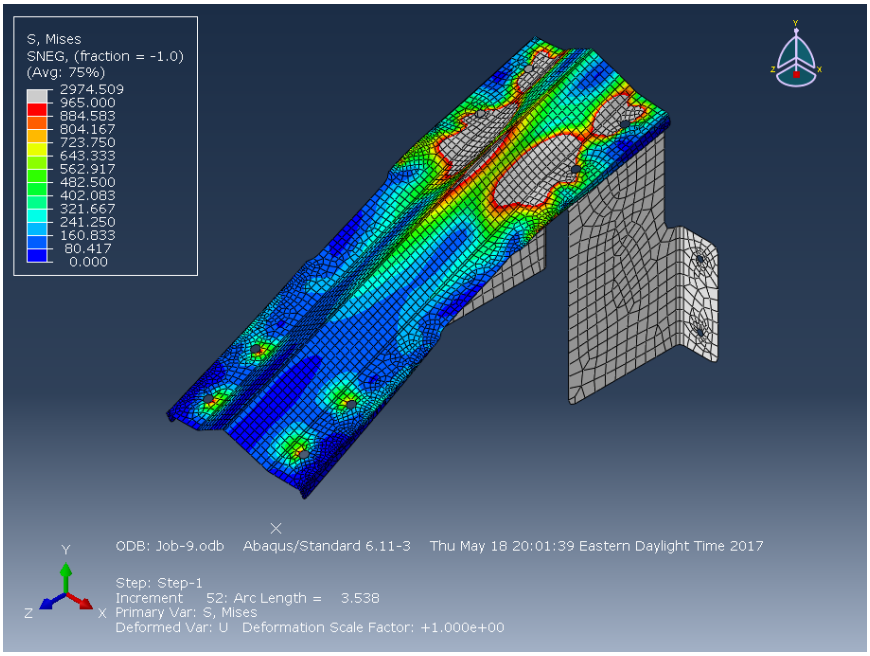

Figure 8.6: Stress distribution on the clicker bracket for design iteration 1.

Figure 8.7: Stress distribution on the clicker bracket for first design iteration.

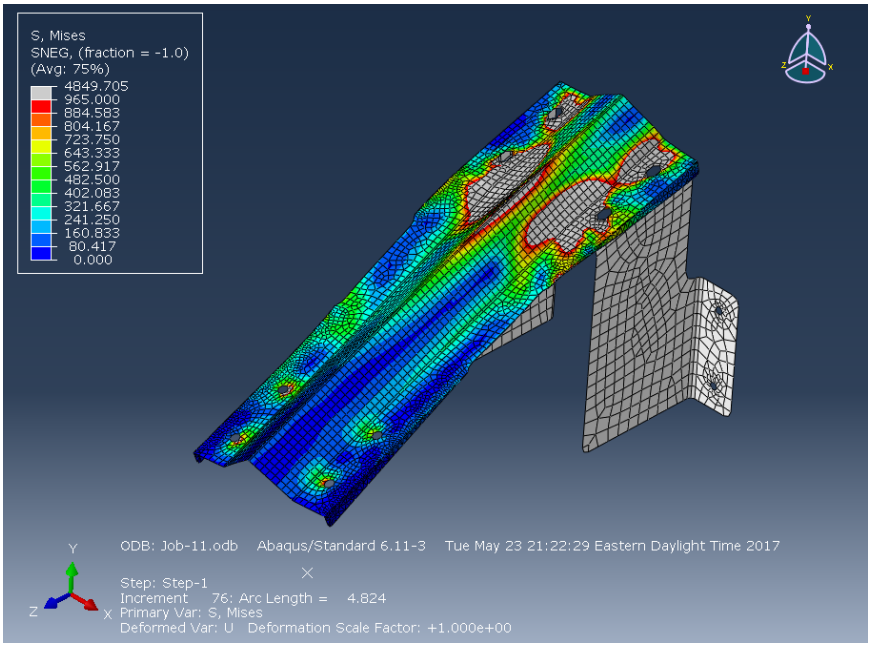

Figure 8.8: Stress distribution on the clicker bracket for design iteration 1 with 200 N lateral load.

figure 8.6. It is observed that the stress levels are beyond the elastic limit of the part thus might lead the part to plasticly deform. The peak stress at on the part were observed to be $2974.509 N/mm^2$. This high stress concentration might be due to stress singularities which have to be verified experimentally. If the stresses were beyond the elastic limit, the part will encounter with localized plastic deformation which will be clear and evident in experimental testing. Also, the stress values obtained from FEA are just an estimate and may not represent actual stress values.

By considering the free play and offset loading on the Instron test machine, a lateral load of 200 N was applied in the x direction of Abaqus axis system along with 1000 N load in y direction. The stress distribution and the load-displacement curve for the same are shown in the figure. It can be observed that the critical buckling load drops down to 919.673 N.

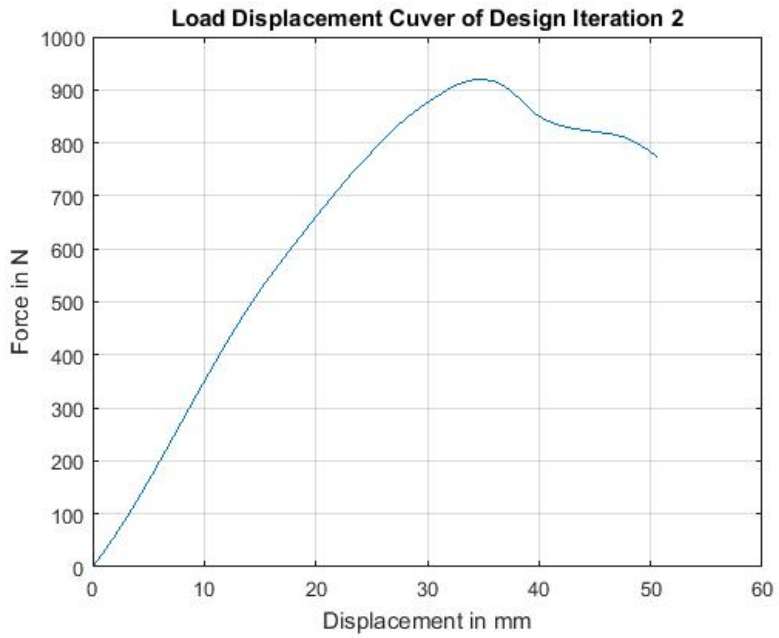

Figure 8.9: Stress distribution on the clicker bracket for first design iteration with 200 N lateral load.

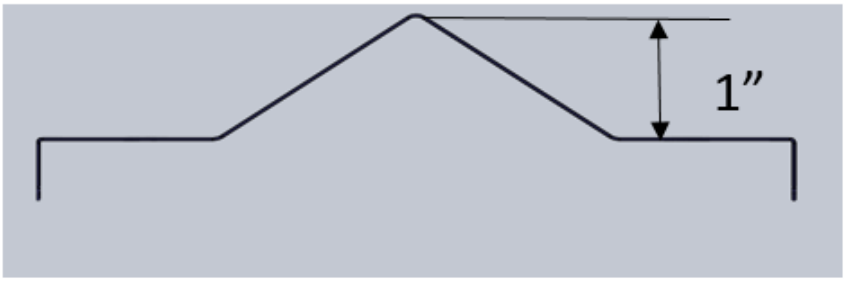

Figure 8.10: Cross sectional view of clicker bracket highlighting the hill height.

8.4 Experimental Test Results

8.4.1 Design 1

Description of the test specimen

Test specimen for the first design is developed. Over all length of clicker bracket is 392.4 mm (15.5 in.). The main design parameter which is of interest is called as

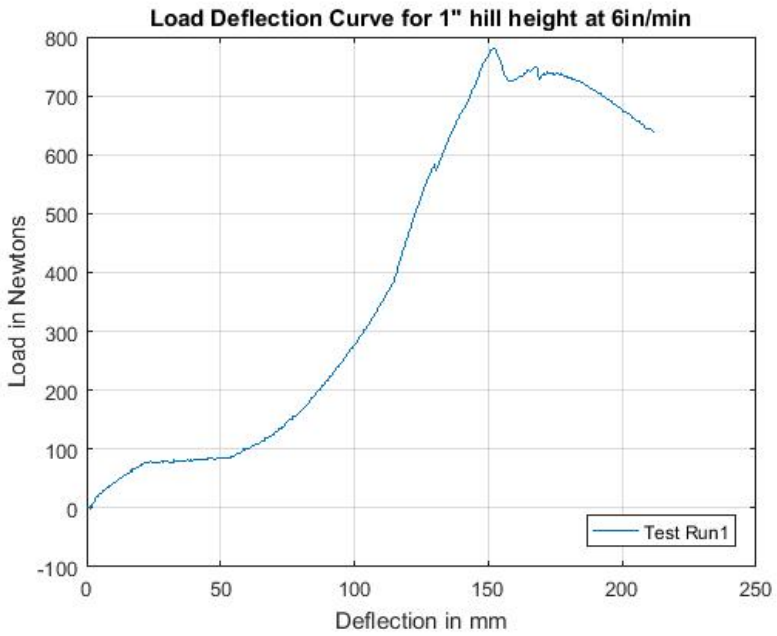

Figure 8.11: Load Deflection data of Design 1 for a strain rate of 6in./min.

the hill height shown in Figure 8.10 as 1 in. (25.4 mm).

Test Method

Every test specimen is tested at two different strain rates, 50.8 mm/min (2 in./min) and 152.4 mm/min (6 in./min), to record critical buckling load at multiple strain rates. A load deflection graph is obtained after every test, which would be interpreted to tell the critical buckling load of the component. When the part buckles there is a sudden drop in the reaction load measured by the load cell without significant change in deflection.

Test Results

The figure 8.11 which shows the result of design 1 which was loaded at a rate of 6 in./min. From the graphs it can be interpreted that there is no significant drop in the load after the limit point. Also, it was observed that specimen have plasticly deformed, meaning the part has failed.

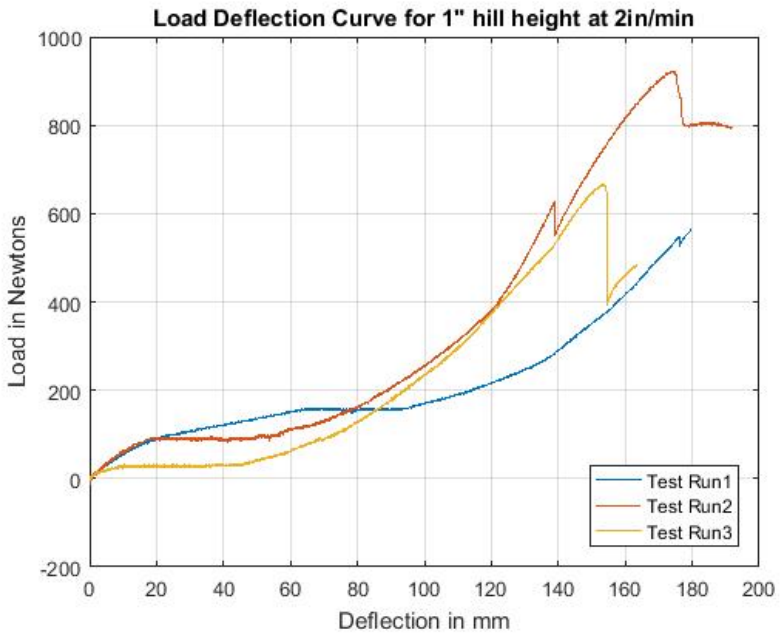

Figure 8.12: Load Deflection data of Design 1 for a strain rate of 2in./min.

Figure 8.13: Deformed shape of the parts after the buckling test. Top sample shows loading rate at 6in./min. Bottom sample shows loading rate at 6 in./min.

The test was repeated on a new specimen, but was loaded at 2 in./min. From the graph shown in figure 8.12 which shows the load deflection curve of the same specimen for multiple tests. It is observed that the graphs do not show repeatable results, because the parts have plasticly deformed after each test run. The deformed test samples are shown in the figure 8.13. From the results obtained though not repeatable, lowest buckling load was observed at 659.4 N. This is in close relation with the buckling load obtained from the finite element analysis which is 919.673 N. A correlation factor (CF) between finite element analysis and experimental results can be drawn for critical buckling load.

$$CF = \frac{-Buckling - Load - from - FEA}{Buckling - Load - from - Experimental - Results} \tag{8.1}$$

$CF = \frac{919.673}{659.4}$

$CF = 1.39$

8.5 Counter Measure Design, Analysis and Testing

The finite element results are in unison with the experimental results in reference to the stress results and critical buckling load. The stresses induced on the clicker bracket are induced due to the high resistance of the bracket from deforming. This phenomenon was proved during the preliminary testing phase. Hence the hill height was reduced to 20.32 mm (0.8 in.) and 15.24 mm (0.6 in.) and finite element analysis of these samples were performed. For the loading conditions a lateral load about X axis of 200 N was applied along the regular 1000 N load. This was to simulate an imperfection loading condition, which was observed in experimental model.

The stress distribution has reduced to $969.442 N/mm^2$, i.e. 67.41% reduction in stress distribution. This reduction might reduce the possibility of plastic deformation of the parts. Also, the critical buckling load reduced to 368.878 N. Hence the predicted buckling load for an experimental results is

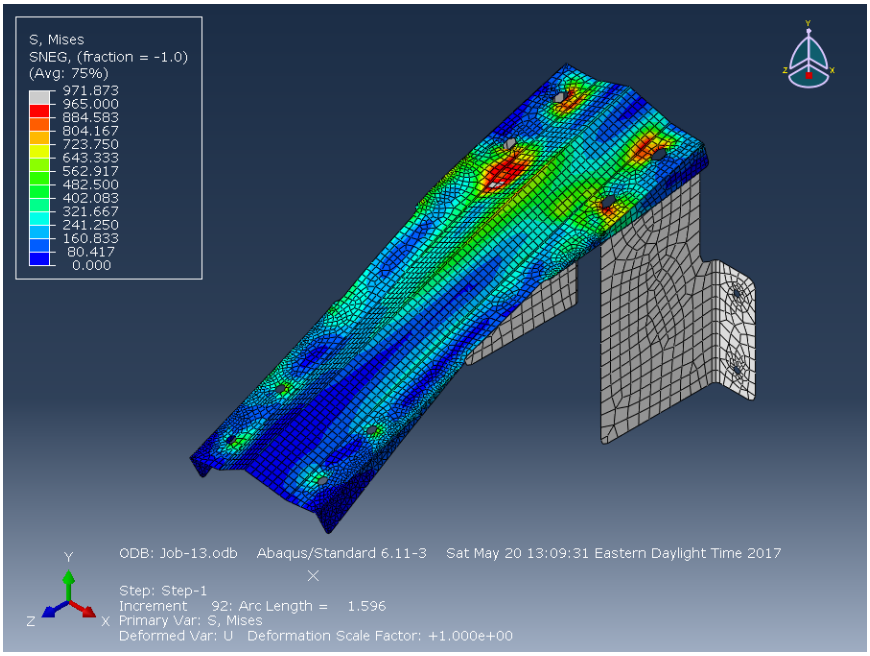

Figure 8.14: Stress distribution on the clicker bracket for design iteration with 0.65 in hill height.

Figure 8.15: Load-Displacement plot of the clicker bracket for design iteration with 0.65 in hill height.

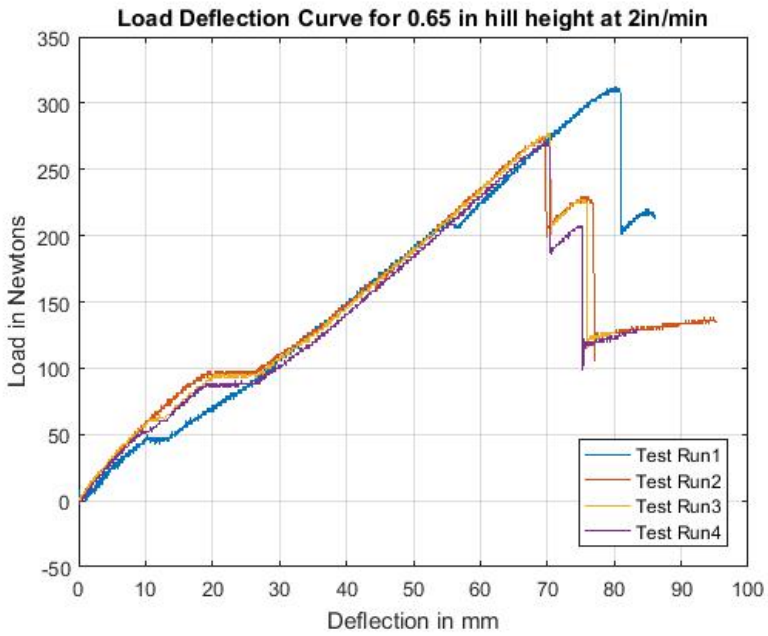

Figure 8.16: Experimental "Load-Displacement" plot of the clicker bracket for design iteration with 0.65in hill height for the test run at 2 in./min.

Predicted Experimental Buckling load = $\frac{368.878}{1.39}$

Predicted Experimental Buckling load = 265.38 N

8.6 Experimental Results for Design Iteration 2

New brackets were manufactured as per the drawings. These brackets were assembled on fixtures of the Instron test machine and the test was run to drive the machine head up, which will apply a downward load on the brackets at the free end. The resultant load deflection diagram for the test runs at 2 in./min and 6 in./min are shown in the figure 8.16 and figure 8.17 respectively.

From the experimental data obtained first critical buckling load for multiple test results are shown in the table 8.1. From the Table it can be observed that the first critical buckling load is observed at 226.86 N. Also, the sample has not plasticly deformed for multiple test runs at various loading rates. These results are in perfect correlation with the finite element model developed, through which buckling load first

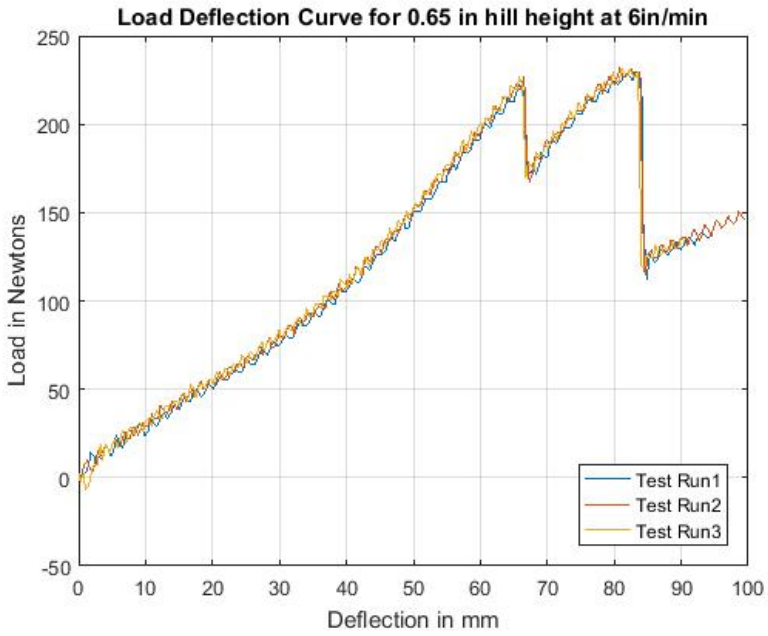

Figure 8.17: Experimental "Load-Displacement" plot of the clicker bracket for design iteration with 0.65 in hill height for the test run at 6 in./min.

Table 8.1: Experimental data of the first critical buckling load for multiple tests on a sample

S.No	1st Critical Buckling Load
1	310.04
2	272.23
3	279.35
4	269.87
5	229.31
6	231.31
7	226.86

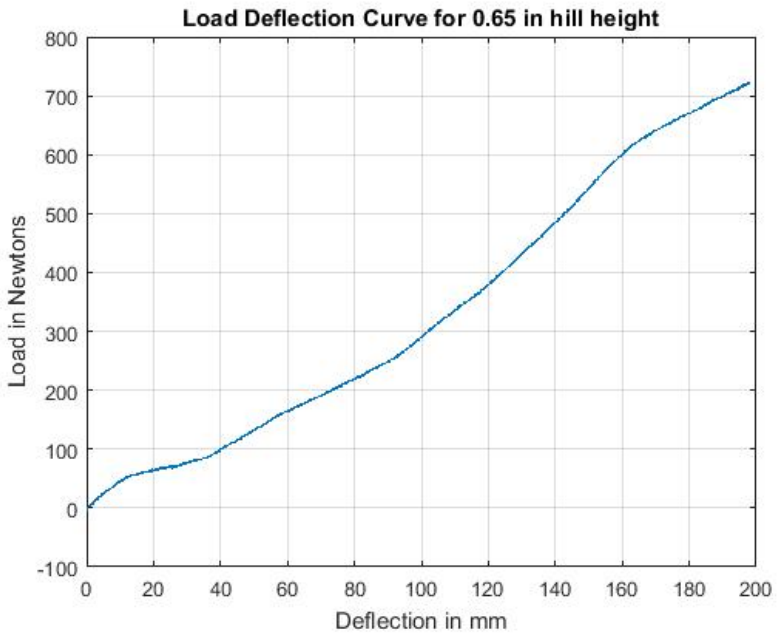

Figure 8.18: Experimental "Load-Displacement" plot of the clicker bracket for design iteration with 0.65in hill height pulled in upward direction.

critical buckling load was estimated as 261.2 N. Stress distribution results in FEA show a drastic reduction in stresses at the rear support of the clicker bracket which was observed experimentally.

8.7 Upward Loading

The second and one of the most important criteria is that the parts should not fail when the operating load are applied in positive Z direction. This test has been performed on the Instron test machine. Test head of the machine is driven in downward direction by holding the free end. This simulates pull up condition of the bracket. The results obtained for the same are shown in the figure 8.18.

The effective stroke length of the machine after installing the strut arm to apply load and the custom made fixture is just 177.8 mm (7 in.). To test the bracket stiffness in +z direction, bracket does not fail for a load upto a load of 943.76 N after which the machine hits emergency stop as it ran out off travel.

The design requirements state that 3 brackets will be operating under an average load of 860N. This accounts up to approximately 290 N for each bracket. If the brackets were to fail at 943.76 N, the factors of safety on the brackets are 3.2, which makes it a confident design to proceed forward.

CHAPTER 9: FINAL DESIGN AND CONCLUSION

9.1 Final Design

The test results of the parts made from the drawings in appendix XXX having hill height of 15.24 mm (0.6 in.), fulfill all the requirements addressed in problem statement. Also, an elaborative manufacturing method was developed to ensure that parts are easy to be manufactured in mass production environment.

9.2 Conclusion

The objective of this thesis was to design a "Clicker Bracket" which exhibits snap-through buckling behavior and collapse beyond a threshold load, and retract back to it's original shape without any plastic deformation. Such a bracket for a structural member can reduce the possibility of the failure of brittle and fragile parts which are a part of the system in which brackets work in. The proposed design was successfully able to solve the problems listed in the problem statement. The problems that were addressed through this thesis project are

- Controlled buckling in the Z direction to avoid transmitting of load to a weaker component.
  - This was achieved by designing a bracket whose base stiffness would support the operating loads and buckle beyond a threshold load of approximately 226 N or 56 pounds.
  - Working proof of such a functionality was estimated using Static Rik's method available in Abaqus Finite Element Analysis tool and validated

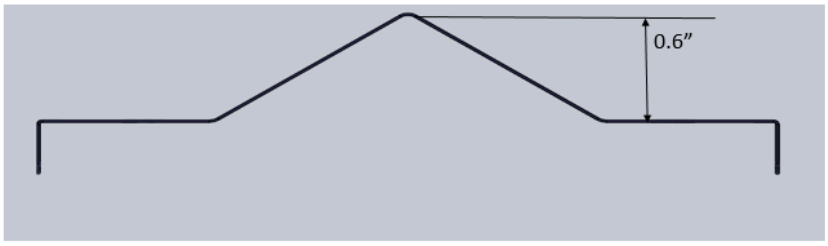

Figure 9.1: Sectional view of the final proposed design

experimentally.

- Bracket should not plasticly deform under the load application in buckling direction
  - To ensure that part does not plasticly deform, FEA tool was used to approximately estimate the stress distribution on the structure. For the initial design the stress distribution was observed to be beyond the yield strength criteria.
  - To validate the results the parts were tested on Instron machine to find severe plastic deformation.
  - Multiple simulations were run using FEA tool, by reducing the section modulus of the whole part.
  - A satisfactory stress distribution was obtained for the design parameter value of 15.24 mm or 0.6 in as shown in the figure 9.1.
- A development request of simple, easy to manufacture and cost effective component was developed which increases the value of the over all system for its unique functionality.

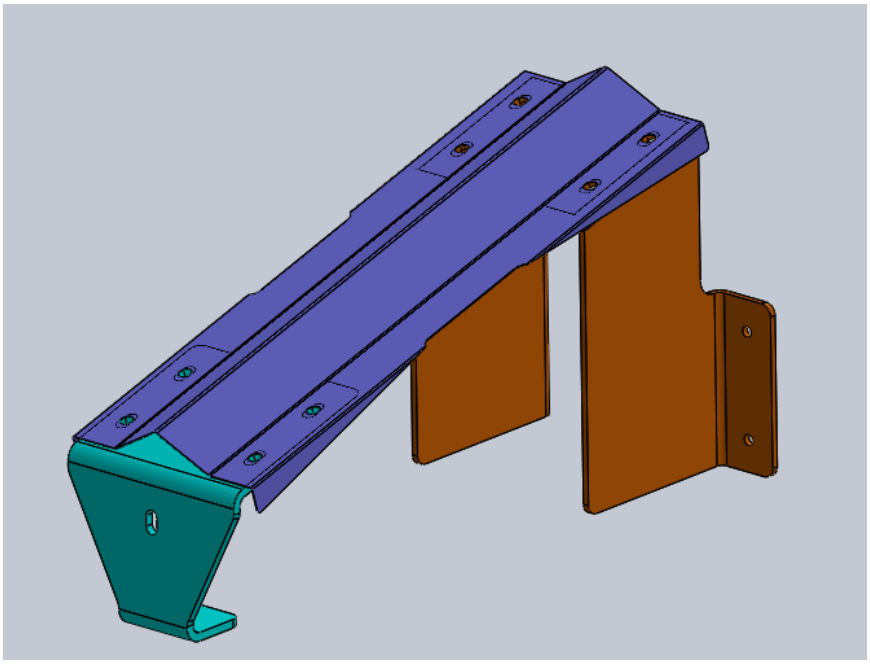

Figure 9.2: Final proposed design

9.3 Applications and Future Scope of Work

Application of controlled buckling finds its applications in major automotive applications.

9.3.1 Applications of Controlled Buckling

- Development of automotive low speed crash structures which buckle at low speed crash and can be reset to their original shape with minor repair.
- Development of skid pads for automotive use. Long thin sheets can be designed as under body skid pad for high performance automobiles with very low ground clearance. Such skid pads deform when they come in contact with a kerb and come back to their original shape under their regular operating conditions.

9.3.2 Short Comings and Future scope of work

The developed finite element model and experimental apparatus fail to determine the total collapse of the structure beyond first and second buckling points. The finite element model solver diverges after the critical buckling load due to involvement of higher contact and insufficient nonlinear material properties. Also the experimental apparatus can be improved to create enough stroke length to test the buckling mode in +z direction.

To overcome all such short comings a robust finite element model can be developed to clearly predict the behavior of the component after first buckling mode. Such a model should be able work under a time dependent loading to predict buckling behavior.

On a final note, though the models and experiments do not clearly predict post buckling behavior, they give an accurate estimate of the first critical buckling load which cannot be obtained by a simple eigenvalue analysis.

BIBLIOGRAPHY

[1] B. S.-S. Sheet, "Strip, and plate: Astm a 240/a 240m or astm a 666," *Type 301L*.

[2] Lincoln Elctric Cutting Systems, *Operator's Manual, Torchmate Classic 4x8*, 2015.

[3] I. Predictive Engineering, "Linear and Nonlinear Buckling Analysis and Flange Crippling," tech. rep.

[4] C. A. Felippa, "Linearized prebuckling: Examples and limitations." http://www.colorado.edu/engineering/cas/courses.d/NFEM.d/NFEM.Ch31.d/NFEM.Ch31.index.html, 2016. [Online; accessed 22-May-2017].

[5] N. Vasios, "Nonlinear analysis of structures, the arc length method: Formulation, implementation and applications," 2015.

[6] E. Riks, "An incremental approach to the solution of snapping and buckling problems," *International Journal of Solids and Structures*, vol. 15, no. 7, pp. 529–551, 1979.

[7] Instron Corporation, *Instron Model 4400, Universal Testing System*, 1995.

[8] K. Hibbitt and Sorensen, *ABAQUS/CAE User's Manual*. Hibbitt, Karlsson & Sorensen, Incorporated, 2002.

[9] S. Novoselac, T. Ergić, and P. Baličević, "Linear and nonlinear buckling and post buckling analysis of a bar with the influence of imperfections.," *Tehnicki vjesnik/Technical Gazette*, vol. 19, no. 3, 2012.

[10] M. Sheidaii, G. Parke, K. Abedi, and A. Behravesh, "Dynamic snap-through buckling of truss-type structures," *International Journal of Space Structures*, vol. 16, no. 2, pp. 85–93, 2001.

[11] Wikipedia, "Buckling — Wikipedia, the free encyclopedia." http://en.wikipedia.org/w/index.php?title=Bucklingoldid=779572928, 2017. [Online; accessed 22-May-2017].

[12] S. Sumirin, N. Nuroji, and S. Besari, "Snap-through buckling problem of spherical shell structure," *International Journal of Science and Engineering*, vol. 8, no. 1, pp. 54–59, 2015.

[13] M. A. Crisfield, "A fast incremental/iterative solution procedure that handles snap-through," *Computers & Structures*, vol. 13, no. 1-3, pp. 55–62, 1981.